ARCHIVIO ISTITUZIONALE
DELLA RICERCA

Alma Mater Studiorum Università di Bologna
Archivio istituzionale della ricerca

Rapid Fabrication of Electro-Adhesive Devices with Inkjet Printed Electrodes

This is the final peer-reviewed author's accepted manuscript (postprint) of the following publication:

Published Version:
Berdozzi N., Chen Y., Luzi L., Fontana M., Fassi I., Molinari Tosatti L., et al. (2020). Rapid Fabrication of Electro-Adhesive Devices with Inkjet Printed Electrodes. IEEE ROBOTICS AND AUTOMATION LETTERS, 5(2), 2770-2776 [10.1109/LRA.2020.2972838].

Availability:
This version is available at: https://hdl.handle.net/11585/780990 since: 2020-11-17

Published:
DOI: http://doi.org/10.1109/LRA.2020.2972838

Terms of use:

Some rights reserved. The terms and conditions for the reuse of this version of the manuscript are specified in the publishing policy. For all terms of use and more information see the publisher's website.

This item was downloaded from IRIS Università di Bologna (https://cris.unibo.it/).
When citing, please refer to the published version.

(Article begins on next page)

06 October 2024

Rapid Fabrication of Electro-Adhesive Devices with Inkjet Printed Electrodes

Nicolò Berdozzi[1], Yi Chen[3], Luca Luzi[1], Marco Fontana[2],
Irene Fassi[3], Lorenzo Molinari Tosatti[3], Rocco Vertechy[1]

***Abstract*—This paper proposes a procedure for the rapid prototyping and on-demand manufacturing of thin film flexible electro-adhesive devices (EADs) made with a commercial polyimide dielectric layer, inkjet printed interdigitated silver electrodes and blade coated silicone elastomer encapsulation backing. As a proof demonstration, flexible thin-film EADs featuring 9.6 cm^2 active area, 315 µm thickness and 0.7 g weight have been manufactured and tested over different adhering substrates showing peak adhesive shear stresses of up to 56.67 kPa, fast response time (11 ms for initial activation and 0.3 s for full electrification) and little energy requirements (from 1.3 mJ for initial activation to 20 mJ for full electrification and with a subsequent power consumption of about 1 mW for long-term grasp holding). Practical application of the manufactured EADs within a gripper for the grasping and handling of real objects that include a glass bottle, a hollow carbon fiber tube, a cardboard box, a box with thin polypropylene envelope and a polypropylene bottle is also demonstrated.**

***Index Terms*—Grippers and Other End-Effectors, Soft Sensors and Actuators, Electro-Adhesion, Inkjet Printing**

I. Introduction

In applications where fragile, compliant or variable shape objects need to be grabbed, a retention action is typically preferred to a compression force. Technologies for generating retention actions between two mating surfaces can be based on different physical principles, such as vacuum suction, magneto-adhesion and electro-adhesion [1].

In an electro-adhesive device (EAD), prehension forces are generated by exploiting the electrostatic attraction between charged electrical conductors of the EAD and image charges induced on the surface of the adhering object, in combination with mechanical friction. However, as irregular airgaps are always present between the mating surfaces and since no ideal dielectric or electrical conductor really exists in nature, the exact fundamental principles governing the practical response of EADs are not easy to identify, and only coarse models with limited accuracy are available for estimating the prehension actions produced by them [1-4].

Despite the complex physics and although the generated retention pressures might be lower than those produced by vacuum suction and magneto-adhesion, EADs exhibit the following interesting features [1,5]: electrical activation with low energy consumption, as they typically behave as capacitors; minimal effect to the adhered objects, as the electro-adhesive actions vanish very quickly away from the mating surfaces; applicability to a wide range of solid materials that include dielectrics, electrical conductors and porous media; retention performances that are almost independent of device size; operation in a variety of settings such as in air, liquids and vacuo; thin-film embodiment that is very compact and lightweight, enabling them to be conformed to almost any shape and size; intrinsic flexibility and, eventually, deformability that enable to automatically adjust their shape to that of the adhering object.

Investigated in the nineteen-sixties as bonding systems for aerospace applications [2] and as fixtures for part machining [6], as well as thirty years later for the handling of cloths, fabrics and optical micro-components [1,5,7], over the last decade electro-adhesion is receiving an increasing interest in the fields of robotics, especially for the development of grippers [8-11] and climbing robots [12-15].

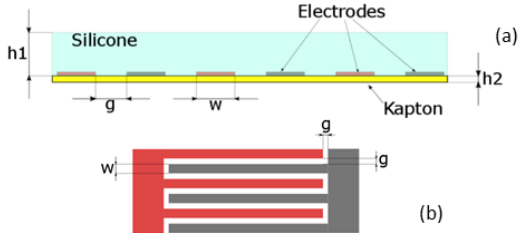

Fig. 1. Electro-Adhesive Device (EAD) cross-section (a) and electrode strip array partial front-view (b).

A classic layout of an EAD with interdigitated electrodes is shown in Fig. 1 [8-15]. It features a layered architecture in which an array of electrode strips, with alternating charge polarity (respectively represented in red and grey), hereafter also called "electrode pair", are encapsulated within two dielectric layers. The lower dielectric layer (colored in

Manuscript received: October 15, 2019; Revised: January 7, 2020; Accepted: January 7, 2020.

This paper was recommended for publication by Editor Cecilia Laschi upon evaluation of the Associate Editor and Reviewers' comments.

This work was supported by the projects Cybersort and FHFFC within the programme "Terzo Accordo Quadro tra CNR e Regione Lombardia".

[1]N. Berdozzi, L. Luzi and R. Vertechy, are with the Department of Industrial Engineering, University of Bologna, Bologna, Italy, rocco.vertechy@unibo.it.

[2]M. Fontana is with the Department of Industrial Engineering, University of Trento, Trento, Italy, marco.fontana-2@unitn.it.

[3]Y. Chen, I. Fassi and L. Molinari Tosatti are with the Institute of Intelligent Industrial Systems and Technologies for Advanced Manufacturing, National Research Council, Milan, Italy, Lorenzo.Molinaritosatti@stiima.cnr.it.

Digital Object Identifier (DOI): see top of this page.

TABLE I
SHEAR STRESS VALUES AT CORRESPONDING APPLIED VOLTAGE WITH CONSTITUTIVE PARAMETERS OF INTEREST OBTAINED FROM LITERATURE

References	Shear Pressure (kPa)	Voltage (kV)	Tested Material	Dielectric thickness (μm)	Electrode gap (μm)	Device materials (Dielectric/Electrode)
Tellez et al. [22]	3.2	4	Steel	1000	7000	PP / Aluminum
Savioli et al. [17]	2	3	Steel	80	2000	PI / Copper
Shea et al. [8]	35	5	Paper	50	500	Silicone / Silicone + Carbon Black
Ruffatto et al. [16]	62.5	5	Glass	150	600	Silicone / Copper
Guo et al. [11]	1.4	4.8	Acrylic plate	200	3000	Silicone / Conductive Silicone
Koh et al. [4]	2.2	10	Glass	90	1200	Cellulose Acetate / Aluminum
Mahmoudzadeh et al. [19]	7.5	5	MDF	60	400	Silicone / Copper
Dadkhah et al. [18]	1.6	5	Drywall	25	400	PI / Copper
Gu et al. [12]	1.12	5	Release paper	20	-	PI / Copper
Ritter et al [23]	1.35	3.5	Aluminized PET	25	-	PI / Aluminum
Choi et al. [24]	15	1	Metal	20	1000	WPU / Copper

yellow), hereafter also called “main dielectric layer”, is the one in contact with the adhering object; it dominantly affects the prehension pressure mostly through its thickness, dielectric strength, electrical permittivity and resistivity. The upper dielectric layer (colored in cyan), hereafter also called “backing”, isolates the electrodes from the environment, increases the breakdown voltage of the device (hence, the maximum prehension pressure) and may be employed to bond the EAD to a host structure when necessary.

The backing might be stiff [16,17] or flexible and, in some cases, even stretchable [8,15]. Since prehension forces are strongly affected by the contact area between the EAD and the object, the choice is driven by application requirements, which also include device resiliency. While for flat items (such as plates or plies) a planar and stiff backing might work, in case the adhering objects have a variable shape or rough surfaces, a flexible or stretchable backing is likely to be a better option, as this makes the EAD to adapt its shape to the item surface, thereby reducing the presence of air gaps and increasing the contact area. The use of flexible and stretchable backing however complicates EAD fabrication, as this requires the handling of thin flexible or stretchable films, which is more difficult than manipulating stiff wafers.

As regards device design, different layout concepts exist that exploit the same physical principle but are significantly different from an architectural point of view. Depending on the disposition of the electrode pair with respect to the main dielectric layer, EADs can have a uni-layer or a bi-layer configuration [18,19]. Additionally, these architectures can be combined with a micro-structured contact surface [19-21], which however do not necessarily provide an improvement in terms of achieved adhesive force despite the increased manufacturing complexity. It is indeed the right choice of constitutive materials, like a doped dielectric, the more effective means to improve EAD performances [19].

Regarding manufacturing, the arising number of technologies for the fabrication of thin-film multilayered structures have allowed researchers to pursue different approaches for the realization of dielectric layers and electrode pairs. As the manufacturing method controls directly the shape, size and quality of the obtainable features, as well as the employable materials, the specific process adopted for producing an EAD severely influences the attainable prehension performances. The essential part of the procedure is the patterning of electrodes onto the dielectric layers and the deposition of the backing encapsulation layer. Several methods have been proposed in the literature: blade or laser cutting and transferring [8,9,11], blade cutting and lamination [12,22,23]; blade coating, laser ablation and plasma bonding [8]; blade coating and blade cutting [14]; chemical etching and spin or roll coating [16,18,19]; photolithography and dip coating [24]. In these processes: copper, aluminum and conducting silicone rubber have been mostly used for the electrodes; polypropylene (PP), polyimide (PI), silicone elastomer, waterborne polyurethane (WPU) and cellulose acetate have been mostly used for the dielectric layers.

Regarding performance, the major key index to be used for quantifying the efficacy of an EAD is the electro-adhesive shear stress (ESS), which indicates the limiting tangential force per unit of active prehension area that can be applied to the adhered object before the occurrence of sliding. Indeed, EADs show far larger resistance to shearing actions rather than to normal and peeling forces [8,12]. ESS values reported in the literature typically range between 1 kPa and 10 kPa, with only a few works having reached values close to 50 kPa and above, and are highly dependent on the geometry and material of both EAD and adhering object. Exemplary results attained in previous works by EADs made with different materials and grabbing different substrates are summarized in Table I.

In this context, this work describes the development and characterization of thin-film flexible EADs made with a commercial PI film as dielectric layer, inkjet printed interdigitated silver electrodes and blade coated silicone elastomer backing. Inkjet printing has the following advantages over the previous described approaches:

- it is a non-contact, mask-less and master-less process, which enables the easy patterning of electrode traces having complex geometry (but also of dielectric layers) with high resolution and repeatability, while leaving the minimal effect on the printed substrate;
- it makes it possible to employ a wide range of materials as the conductive and dielectric layers to best adapt to different application requirements;
- it adapts well to a wide range of production scales, that include prototyping, on-demand fabrication and large-scale industrial production;
- it is well suited for the realization of a wide variety of

device geometries having different sizes;
- it is a relatively green process, that involves minimal waste of material and minimal use of corrosive chemicals.

After having described the manufacturing process and the prehension performances of the developed EADs over different substrates, where ESSs of up to 56.67 kPa and 45.78 kPa are demonstrated respectively for coated polyethylene terephthalate (PET) and aluminized PI substrates, the paper describes one of their possible uses in a simple, though very effective and versatile, gripper for the handling of objects with different geometry and of different material.

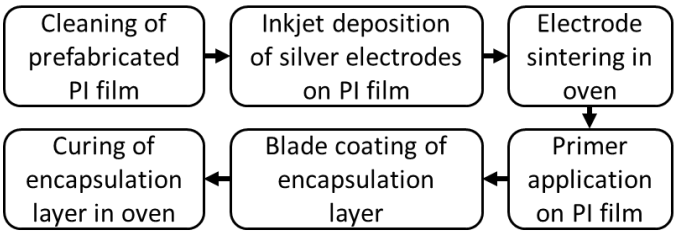

Fig. 2. Phase sequence of the process proposed for EAD manufacturing.

II. Design and Fabrication

In this work, EADs are manufactured by patterning the electrode pair via inkjet printing on a pre-fabricated dielectric film and by using blade coating for the deposition of the backing electrode-encapsulation layer. A diagram describing the different phases of the overall manufacturing process is shown in Fig. 2.

The uni-layer design shown in Fig. 1 is considered for a first demonstration of the proposed fabrication method and for the evaluation of the prehension performances attained by the manufactured EADs. With little modifications, this method could also be adapted for the fabrication of bi-layer architectures, as well as to realize a micro-structured contact surface.

Due to quick availability, ease of handling, adequate dielectric properties and mechanical flexibility, PI is chosen as the main dielectric layer and silicone elastomer is chosen for the backing. A silver ink for flexible electronics is used for the electrodes.

An exemplary EAD manufactured via the proposed method is shown in Fig. 3. According to Fig. 1 and 3, the considered EAD geometry is the following: electrode width and gap, $w = 400$ µm and $g = 300$ µm; main dielectric thickness, $h_2 = 25.4$ µm; backing thickness, $h_1 \approx 290$ µm; EAD active length and width, $L = 24$ mm and $H = 40$ mm; EAD active area, $A = L \times H = 9.6$ cm^2. With a thickness of around 315 µm and a weight of 0.7 g, the manufactured EAD is very flexible, compact and lightweight.

Manufacturing of the EAD depicted in Fig. 3 requires about 112 minutes for a single device, plus a further 16 minutes per additional unit up to a maximum of 24 units that can be fabricated altogether.

A total of 7 nominally identical EAD specimens have been manufactured via the proposed method, which have then been subjected to testing as reported in Sections III, IV and V. Specific details on employed materials and fabrication steps are given in the next subsections.

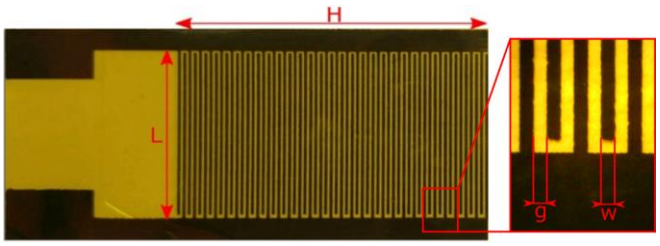

Fig. 3. EAD manufactured via ink-jet printing and blade coating: full device (on the left); detail of the inkjet printed electrode traces (on the right).

A. Main Dielectric Layer

For this first demonstration, a commercial PI film (Caplinq PIT1N/210) provided in rolls with a thickness of 25.4 µm and a width of 210 mm is chosen as the main dielectric layer and as the printing substrate for electrode patterning. A pre-fabricated film has been preferred to a custom realization to guarantee the uniformity of substrate thickness and material properties, which is fundamental for the achievement of high and reliable performances that are consistent across all the manufactured EAD specimens. In terms of relevant material properties, the considered PI film features: a relative dielectric constant of 3.9; a dielectric strength of 236 MV/m; a volume resistivity of around 1 MΩ·cm; a continuous use temperature of up to 260 °C.

B. Electrode Pair Fabrication

A drop-on-demand inkjet printer (MicroFab Jetlab® 4xl) with a 50 µm diameter nozzle is used for electrode pair deposition onto the PI film according to the desired pattern.

A commecial ink (Anapro DGP 40LT-15C), made with silver nanoparticles dispersed in a triethylene glycol monoethyl ether solvent, is used as electrode material due to its good compatibility with plastic film substrates, low volume resistivity (around 12 µΩ·cm) and relatively low curing temperature (in the range 120 °C and 150 °C).

The inner side of PI film roll is chosen as the printed surface. Prior to ink deposition, the PI film is cleaned with dry cleanroom paper to remove dust fibers. To reduce the mobility of dispensed ink droplets, thus to decrease the risks of defects in electrode pattern that may give rise to short circuits, the printing platen is kept at 50 °C to facilitate solvent evaporation right after the droptles reach the PI film. Printing of the considered pattern takes about 16 minutes. Once printing is finished, the PI film is transfered in an oven, where it resides for about 45 minutes at 120 °C to enable the sintering of the silver nanoparticles.

C. Backing Encapsulation Layer Fabrication

An automatic thin-film deposition system with vacuum bed and micrometer adjustable blade applicator (TQC Sheen AB3655 and VF1823) is used for the casting of the backing encapsulation layer over the PI film on the side where the electrode pattern has been printed. This process has been selected due to its simplicity, speed and reliability.

A commercial two-component liquid silicone elastomer (Wacker Silpuran® 6000/05) is chosen as the main material. A mixture of the two parts of the silicone elastomer (part A and part B) and a silicone solvent (Dow DOWSIL™ OS-2) with a weight ratio of 5:5:8 is firstly prepared. The solution is homogenized in a planetary-centrifugal mixer (Thinky ARE-250) for 2 minutes at 2000 rpm and then degassed for another 2 minutes at 2000 rpm. The degassing step is fundamental to remove entrapped air bubbles in the mixture which could cause premature dielectric breakdown of the encapsulation layer and, thus, reduce the prehension performances of the manufactured EADs. Prior to solution deposition, the electroded PI film surface is treated with a primer (Dow DOWSIL™ 1200 OS Primer) in order to improve both the quality and speed of adhesion between PI and silicone elastomer. Treatment is performed by manually applying a thin layer of primer through a clean stick with lint-free foam pad and then leaving it cure in air. This step requires about 15 minutes. Solution deposition is made with the automatic applicator with a blade height adjusted to 700 µm to obtain a silicone layer of around 290 µm ± 10 µm, as a thickness reduction of around 60 % occurs after solvent evaporation that is done in ambient conditions. Deposition with the automatic applicator requires about 2 minutes. As a last step, vulcanization of the deposited silicone elastomer is performed in an oven for 30 minutes at 85 °C.

III. Experimental Setup and Test Procedure

Quantitative validation of the manufactured EAD specimens is accomplished in terms of the ESS developed over different adhering objects at different levels of electric potential difference (voltage) applied to the electrode pair.

In order to assess the EAD performance in a reliable and replicable manner, the following commercial thin films, with controlled material properties and geometry, have been considered as adhering object/substrate samples:

- 25 µm PI film (Caplinq PIT1N, inner side of roll);
- 75 µm PI film (Caplinq PIT3N, inner side of roll);
- Aluminized PI Film (Caplinq PIT1N-ALUM, with 25 µm PI thickness and 0.1 µm sputtered aluminum coating, aluminum side);
- PET film (JetStar Standard Inkjet Film, with a thickness of 130 µm, non-coated side);
- Coated PET film (JetStar Standard Inkjet Film, with a thickness of 130 µm, coated side).

Beside evaluating the ESS-voltage relationships, the electrical properties and the time response of an EAD during an operation cycle are also investigated to provide an indication of the self-sensing capabilities of the device as well as its operational energy requirements.

A. Experimental Setup for ESS Measurement

Fig. 4 and 5 respectively show the schematic and real arrangement of the experimental setup conceived for ESS measurement.

In the setup, which resembles the apparatus described in the ISO 8295 standard [25] for the determination of the friction coefficient for plastic film and sheeting, the mating surfaces of EAD specimen and material sample are placed together in plane contact and under uniform contact pressure. The EAD specimen is kept fixed to ground on a horizontal plane, whereas the material sample is attached to a sled that is constrained to move in the horizontal direction by a linear guide and equipped with a loadcell (NS-WL1-10kg) to enable measurement of the tangential force exchanged between the mating surfaces. Electrical activation of the EAD is performed with a high voltage supply (ULTRAVOLT® 40A24 or 20HVA24-bp1), which also enables to measure voltage and current across the EAD specimen. Control and data acquisition are performed at a sampling frequency of 1 kHz by a Beckhoff real-time controller (CX5140-0125 with I/O modules EL3356, EL3104, EL4732) under TwinCAT 3 environment.

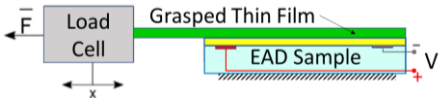

Fig. 4. Schematic of the test-bench employed for ESS measurement.

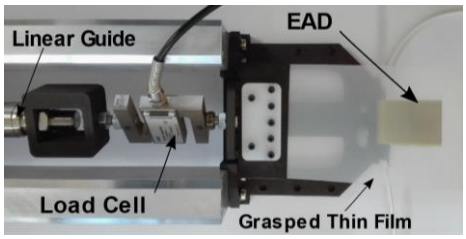

Fig. 5. Picture of the test-bench employed for ESS measurement.

B. Testing procedure

Before ESS experiments, capacitance measurement of each of the seven EAD specimens is performed at 20 Hz with a LCR meter (Rohde & Schwarz HM8118). Besides providing an indication of the energy required for EAD operation, the variation in capacitance across different EAD specimens can be used to quantify the consistency of the procedure proposed here for their manufacturing.

For ESS measurement, first the material sample under test is manually placed over the EAD specimen. Second, to reduce the variability introduced by the human operator (in particular, the motion and force applied during mating surface alignment), a pre-load of 1 kg is applied above the testing area before electrical activation. After charging the EAD specimen to a desired voltage level, the pre-load is removed and a weight of 42 g is left on top of the testing area to provide a minimum normal contact pressure comparable to that suggested in the ISO 8295 standard [25]. Then, the thin film sample is pulled through the linear guide away from EAD specimen and the exchange shear force is recorded till slipping occurs. For each EAD specimen and material sample, tests are performed with voltage levels increasing from 0 kV to 5 kV with 1 kV step. Before testing a new EAD specimen or material sample, the contact surface is cleaned with propanol in order to remove dust and grease and then dried with cleanroom paper. After the discharging phase of each test, any residual surface charge is removed from the mating

surfaces of both EAD specimen and film sample with a grounded aluminized PI film.

To explore the performance limits of the manufactured EADs, additional ESS tests have also been conducted on two EAD specimens, one over the coated PET sample and one over the aluminized PI sample, with non-constant increasing voltage steps till electrical breakdown of the EAD specimen.

IV. Results

This section reports the results of the experiments conducted on the manufactured EAD specimens.

A. EAD Capacitance

Table II shows the results of the capacitance measurements performed on seven nominally identical manufactured EAD specimens under the following conditions: exposed to free air, in contact to the coated PET sample, in contact to the aluminized PI sample.

The limited value of the standard deviation (SD), especially for the free-air case, indicates that the proposed fabrication procedure can be considered repeatable. The relative increase in the SD value when the EAD is in contact with an adhering object may be due to entrapped air between the mating surfaces, as this influences the effective capacitance of the system made by EAD specimen and film sample.

The significant increase in the mean value of capacitance when the EAD is in contact to an adhering substrate (a 2.4 increase for coated PET and a 3.6 increase for aluminized PI with respect to the free-air cases) indicates that the EAD features an intrinsic self-sensing ability that can be exploited to detect contact with a neighbor object.

TABLE II
MEASURED CAPACITANCE OF THE MANUFACTURED EAD SPECIMENS: MEAN AND STANDARD DEVIATION (SD) VALUES EVALUATED FOR SEVEN NOMINALLY IDENTICAL EAD SPECIMENS

	EAD Capacitance		
	in Free Air	on Coated PET	on Aluminized PI
Mean (pF)	28.8	70.7	105.67
SD (pF)	1.04	5.54	7.37
SD/Mean (%)	3.61	7.83	6.97

B. Electro-Adhesion Shear Stress (ESS)

Fig. 6 summarizes the measured ESS results obtained on the seven manufactured EAD specimens, over the five different adhering film samples, for different EAD activation voltages. The error bars are the standard deviation of the measured ESS among different EAD specimens. Results highlight a significant increase in ESS with applied voltage, with the increase being more than linear and depending on substrate material and thickness. For activation levels higher than 1 kV, the largest ESS values are obtained for coated PET and aluminized PI. No significant trend is instead observed for lower voltages as, for these cases, the contribution due to electrostatic attraction is very modest with respect to that due to the 42 g weight. The thin PI film seems to adhere better than its thicker counterpart. As compared to Table I, which summarizes well-known and recent results in the literature, the ESS values reported here are among the highest attained; in particular: one order of magnitude better than those recorded for existing EADs with a similar PI main dielectric layer; comparable to those recorded for existing EADs with a silicone elastomer main dielectric layer, which is known to have a higher interfacial friction (and adhesion at no voltage) than PI on the considered film samples.

To assess maximum ESS performance, additional tests on coated PET and aluminized PI samples have been conducted with the activation voltage increasing from 1 kV till EAD rupture due to dielectric breakdown, which occurred in the backing silicone layer respectively at 8.3 kV and 7.6 kV. Results are reported in Fig. 7, which shows a saturation of the measured ESS for both the adhering substrates. Measured peak ESS values are 45.78 kPa at 6 kV for Aluminized PI and 56.67 kPa at 7 kV for coated PET, which are very promising values, especially considering that the recorded saturation may leave space for improvement. A closer examination on the considered EAD specimens indeed revealed that some electrode traces have been burnt away for activation voltages higher than 6 kV. Although these burnt-away electrodes did not short-circuit the EAD specimen before its global breakdown, they might have compromised its prehension performance, as represented by the plateau.

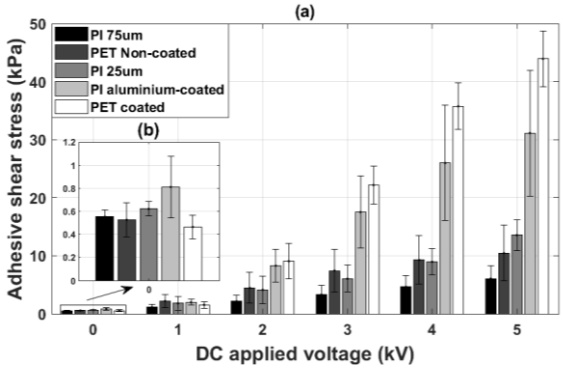

Fig. 6. Measured electro-adhesion shear stress (ESS): mean (column) and standard deviation (error bar) values evaluated for seven nominally identical manufactured EAD specimens. (a) ESS vs EAD activation voltage for different film samples. (b) zoom for the case with no voltage applied.

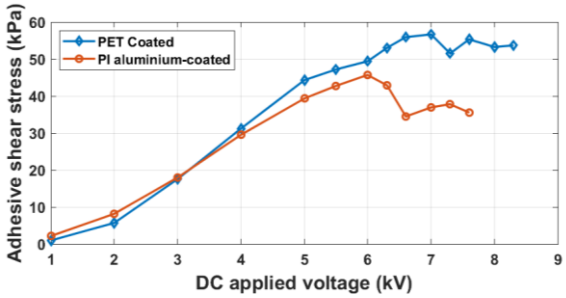

Fig. 7. Electro-adhesion shear stress (ESS) vs applied voltage for coated PET and aluminized PI till EAD specimen breakdown.

C. Energy and Power Consumptions

Fig. 8 reports the full status of one of the manufactured EAD specimens over one cycle of operation during the ESS tests when grasping the aluminized PI substrate at 5 kV. In particular: Fig. 8a shows the evolution of the voltage applied

between the EAD electrodes and the current flowing through them; Fig. 8b shows the power and energy supplied to the EAD; Fig. 8c shows the shear force measured by the loadcell in the setup of Fig. 4 and 5. As the employed power supply (Ultravolt 20HVA24-bp1) has a rated current of 50 µA, the current immediately saturates during charging, which occurs at 0.4 s; this also limits the maximum power absorbed by the EAD specimen below 0.27 W. Despite the initial electrical activation of the EAD requires about 11 ms and 1.3 mJ, which are consistent with the capacitance values reported in Table II, a significant amout of current needs to be suplied for about 0.3 s and with an energy expenditure of about 20 mJ for proper material electrification (namely, for the current to settle after the asymptotic decay shown in Fig. 8a due to dielectric absorption and sweep of mobile ions to the electrodes). After full EAD electrification, maintenance of the grasping requires about 1 mW to compensate for the current leakage that is due to the finite resistivity of the employed real dielectrics. Although barely visible, the loss of grasp that occurs around 4.7 s causes a current flow from the EAD to the power supply with a little return of energy.

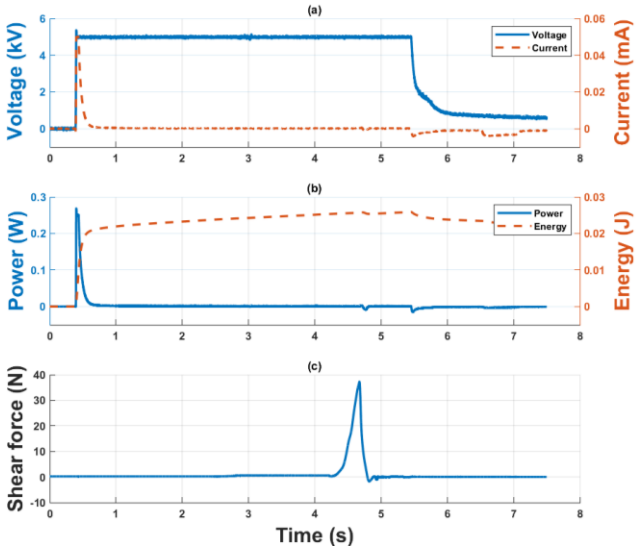

Fig. 8. Status of EAD during one cycle of charging and discharging: (a) voltage and current history from power supply monitoring signals; (b) estimated power and energy history; (c) force history from loadcell signal.

V. Gripper Application

To validate the manufactured EAD specimens in the manipulation of common objects, a simple gripper made with two opposite hanging EADs has been realized.

Gripper embodiment along with demonstration of its ability in the grasping of a glass bottle is demonstrated in Fig. 9. In particular, Fig. 9b and 9e show the capability of the manufactured flexible EADs to automatically close around the object to be grasped (in this case a glass bottle) upon electrical activation by using the same electrostatic attraction pressure that generates the retention action. In fact, if the EAD and the object touch in some location (as shown in Fig. 9b and 9c), electrical activation provides a zipping action that makes the EAD flex and lay down on the object surface (as shown in Fig. 9d and 9e) so as to maximize the combined EAD-object capacitance.

Fig. 10 demonstrate instead the ability of the same gripper in the handling of different objects; in particular: a glass bottle filled with water having a weight of 500 g (Fig. 10a and 10b); a hollow carbon fiber tube having a weight of 159 g (Fig. 10c); a cardboard box with a weight of 41 g (Fig. 10d); a box with a thin PP envelop with a weight of 211 g (Fig. 10e); a PP bottle partially filled with propanol having a weight of 52 g (Fig. 10f).

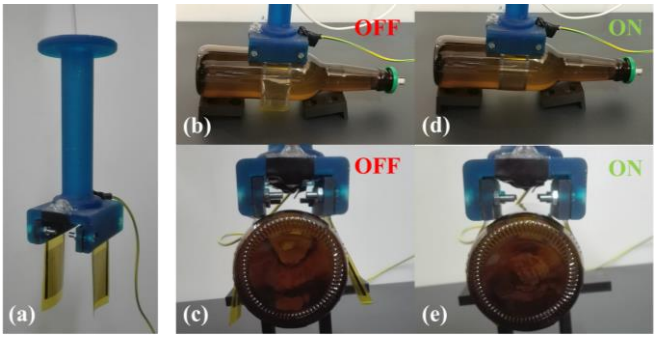

Fig. 9. Simple robotic gripper made with two opposite hanging EADs and its use for the grasping of a glass bottle: (a) gripper embodiment; (b) gripper open under no voltage, lateral view; (c) gripper open under no voltage, axial view; (d) gripper closed after electrical activation, lateral view; (e) gripper closed after electrical activation, axial view.

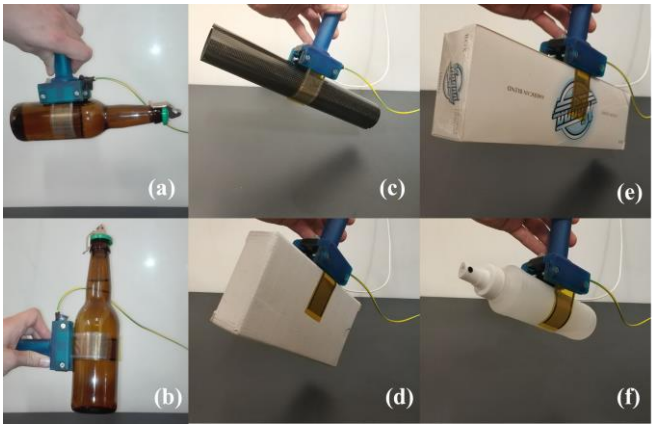

Fig. 10. Simple robotic gripper made with two opposite hanging EADs while handling different objects: (a) a water-filled glass bottle lying horizontal; (b) a water-filled glass bottle lying vertical; (c) a carbon fiber tube; (d) a cardboard box; (e) a box with PP envelop; (f) a propanol-filled plastic bottle.

VI. Conclusions

In this work, a procedure based on inkjet printing and blade coating has been proposed for the fabrication of 315 µm thick electro-adhesive devices (EADs) having a polyimide main dielectric layer, silver interdigitated electrodes and silicone elastomer backing. Requiring about 112 minutes for the production of a single EAD with an active area of 9.6 cm^2, plus a further 16 minutes per additional device up to a maximum of 24 units, the proposed procedure is suitable for the rapid prototyping and on-demand manufacturing of thin-film flexible EADs, and even scalable for large production.

Seven nominally identical EAD specimens have been manufactured with the proposed procedure and then subjected to electrical and mechanical testing.

Capacitance measurements showed a small relative

standard deviation, indicating that the proposed fabrication procedure can be considered very reliable, and a significant dependence on the adhering substrate material, evidencing the inherent ability of EADs in sensing the presence of an adjacent object.

Tangential force tests demonstrated the capability of the manufactured EAD specimens to adhere well to different substrates, though with performances depending on object material and thickness. In particular, the following maximum adhesion shear stresses have been recorded for the EADs operated with an activation voltage of 5 kV: 48.68 kPa on coated polyethylene terephthalate film; 41.99 kPa on an aluminized polyimide film; 16.21 kPa on a 25 µm polyimide film; 15.24 kPa on a non-coated polyethylene terephthalate film; 8.31 kPa on a 75 µm polyimide film. Moreover, peak shear stresses of 56.67 kPa and 45.78 kPa have been respectively achieved for coated polyethylene terephthalate film at 8.3 kV and aluminized polyimide film at 7.6 kV. These values are among the highest reported in the literature for similar EAD and adhering substrate materials. For all tested substrates, adhesion shear stress increased with EAD activation voltage, without globally following the theoretical quadratic law, and showed a significant saturation for activation voltages higher that 6 kV.

Electrical measurement during EAD operation with a 50 µA limited power supply highlighted fast response time, 11 ms for initial activation and 0.3 s for full electrification, and small energy consumption, from 1.3 mJ for initial activation to 20 mJ for full electrification with a subsequent power consumption of about 1 mW for long-term grasp holding.

To validate the practical effectiveness of the proposed rapid fabrication approach and the performance of the manufactured specimens, a simple gripper with a parallel pair of free hanging EADs has been constructed and successfully tested for the grabbing and handling of a variety of objects, including: a glass bottle completely filled with water, a hollow carbon fiber tube, a cardboard box, a box with thin polypropylene envelope and a polypropylene bottle partially filled with propanol.

Beside the capability of lifting and tilting the objects, these tests also demonstrated the efficacy of the electrostatic attraction principle in actuating the flexible EADs within a limited range to make them approach the object and optimally conform to its surface prior to grasping.

REFERENCES

[1] G. J. Monkman, "An Analysis of Astrictive Prehension," *Int. J. Robot. Res.*, vol. 16, no. 1, pp. 1–10, Feb. 1997.

[2] R. P. Krape, "Applications Study of Electroadhesive Devices (NASA Contractor Report: NASA CR-1211) National Aeronautics and Space Administration," 1968.

[3] C. Cao, X. Sun, Y. Fang, Q.-H. Qin, A. Yu, and X.-Q. Feng, "Theoretical model and design of electroadhesive pad with interdigitated electrodes," *Mater. Des.*, vol. 89, pp. 485–491, Jan. 2016.

[4] K. Koh, M. Sreekumar, and S. Ponnambalam, "Experimental Investigation of the Effect of the Driving Voltage of an Electroadhesion Actuator," *Materials*, vol. 7, no. 7, pp. 4963–4981, Jun. 2014.

[5] G. J. Monkman, P. M. Taylor, and G. J. Farnworth, "PRINCIPLES OF ELECTROADHESION IN CLOTHING ROBOTICS," *Int. J. Cloth. Sci. Technol.*, vol. 1, no. 3, pp. 14–20, Mar. 1989.

[6] M. M. Tazetdinov, "Electric fixture arrangements," *Mach. ToolsRussian*, vol. 3, pp. 33–34, 1969.

[7] G. Monkman, "Electroadhesive microgrippers," *Ind. Robot Int. J.*, vol. 30, no. 4, pp. 326–330, Aug. 2003.

[8] J. Shintake, S. Rosset, B. Schubert, D. Floreano, and H. Shea, "Versatile Soft Grippers with Intrinsic Electroadhesion Based on Multifunctional Polymer Actuators," *Adv. Mater.*, vol. 28, no. 2, pp. 231–238, Jan. 2016.

[9] C. Xiang, J. Guo, and J. Rossiter, "ContinuumEA: a soft continuum electroadhesive manipulator," presented at *IEEE International Conference on Robotics and Biomimetics (ROBIO)*, Kuala Lumpur, Malaysia, 2018, pp. 2473–2478.

[10] J. Shintake, V. Cacucciolo, D. Floreano, and H. Shea, "Soft Robotic Grippers," *Adv. Mater.*, vol. 30, no. 29, p. 1707035, Jul. 2018.

[11] J. Guo, K. Elgeneidy, C. Xiang, N. Lohse, L. Justham, and J. Rossiter, "Soft pneumatic grippers embedded with stretchable electroadhesion," *Smart Mater. Struct.*, vol. 27, no. 5, p. 055006, May 2018.

[12] G. Gu, J. Zou, R. Zhao, X. Zhao, and X. Zhu, "Soft wall-climbing robots," *Sci. Robot.*, vol. 3, no. 25, p. eaat2874, Dec. 2018.

[13] S. D. de Rivaz, B. Goldberg, N. Doshi, K. Jayaram, J. Zhou, and R. J. Wood, "Inverted and vertical climbing of a quadrupedal microrobot using electroadhesion," *Sci. Robot.*, vol. 3, no. 25, p. eaau3038, Dec. 2018.

[14] K. H. Koh, M. Sreekumar, and S. G. Ponnambalam, "Hybrid electrostatic and elastomer adhesion mechanism for wall climbing robot," *Mechatronics*, vol. 35, pp. 122–135, May 2016.

[15] H. Prahlad, R. Pelrine, S. Stanford, J. Marlow, and R. Kornbluh, "Electroadhesive robots; wall climbing robots enabled by a novel, robust, and electrically controllable adhesion technology,"presented at *IEEE International Conference on Robotics and Automation*, Pasadena, CA, USA, 2008, pp. 3028–3033.

[16] D. Ruffatto, J. Shah, and M. Spenko, "Increasing the adhesion force of electrostatic adhesives using optimized electrode geometry and a novel manufacturing process," *J. Electrost.*, vol. 72, no. 2, pp. 147–155, Apr. 2014.

[17] L. Savioli, G. Sguotti, A. Francesconi, F. Branz, J. Krahn, and C. Menon, "Morphing electroadhesive interface to manipulate uncooperative objects," presented at the SPIE Smart Structures and Materials + Nondestructive Evaluation and Health Monitoring, San Diego, California, USA, 2014, p. 906129.

[18] M. Dadkhah, D. Ruffatto, Z. Zhao, and M. Spenko, "Increasing adhesion via a new electrode design and improved manufacturing in electrostatic/microstructured adhesives," *J. Electrost.*, vol. 91, pp. 48–55, Feb. 2018.

[19] S. M. J. Mahmoudzadeh Akherat, M. A. Karimi, V. Alizadehyazdi, S. Asalzadeh, and M. Spenko, "A tunable dielectric to improve electrostatic adhesion in electrostatic/microstructured adhesives," *J. Electrost.*, vol. 97, pp. 58–70, Jan. 2019.

[20] R. Dhelika, P. Hemthavy, K. Takahashi, and S. Saito, "Compliant bipolar electrostatic gripper with micropillar electrodes array for manipulation at macroscale," *Smart Mater. Struct.*, vol. 25, no. 5, p. 055037, May 2016.

[21] J. Krahn, A. Pattantyus-Abraham, and C. Menon, "Polymeric electro-dry-adhesives for use on conducting surfaces," *Proc. Inst. Mech. Eng. Part J. Mater. Des. Appl.*, vol. 228, no. 2, pp. 109–114, Apr. 2014.

[22] J. P. D. Tellez, J. Krahn, and C. Menon, "Characterization of electro-adhesives for robotic applications," presented at *IEEE International Conference on Robotics and Biomimetics*, Karon Beach, Thailand, 2011, pp. 1867–1872.

[23] M. Ritter and D. Barnhart, "Geometry characterization of electroadhesion samples for spacecraft docking application," presented at *IEEE Aerospace Conference*, Big Sky, MT, USA, 2017, pp. 1–8.

[24] K. Choi *et al.*, "Quantitative Electrode Design Modeling of an Electroadhesive Lifting Device Based on the Localized Charge Distribution and Interfacial Polarization of Different Objects," *ACS Omega*, vol. 4, no. 5, pp. 7994–8000, May 2019.

[25] *Plastics Film and sheeting Determination of the coefficients of friction*, BS EN ISO 8295:2004, 2004.